Pergamon

Bioorganic & Medicinal Chemistry 10 (2002) 1991–1997

BIOORGANIC & MEDICINAL CHEMISTRY

Synthesis and In Vitro Characterization of a Tissue-Selective Fullerene: Vectoring $C_{60}(OH)_{16}$AMBP to Mineralized Bone

Kelly A. Gonzalez,[a] Lon J. Wilson,[a,*] Wenju Wu[b] and George H. Nancollas[b]

[a]*Department of Chemistry and the Center for Nanoscale Science and Technology and the Laboratory for Biochemical and Genetic Engineering, MS-60, Rice University, PO Box 1892, Houston, TX 77251-1892, USA*
[b]*Department of Chemistry, State University of New York at Buffalo, Buffalo, NY 14214-3001, USA*

Received 18 October 2001; accepted 10 December 2001

Abstract—A tissue-vectored bisphosphonate fullerene, $C_{60}(OH)_{16}$AMBP [4,4-bisphosphono-2-(polyhydroxyl-1,2-dihydro-1,2-methanofullerene[60]-61-carboxamido)butyric acid], designed to target bone tissue has been synthesized and evaluated in vitro. An amide bisphosphonate addend, in conjunction with multiple hydroxyl groups, confers a strong affinity for the calcium phosphate mineral hydroxyapatite of bone. Constant composition crystal growth studies indicate that $C_{60}(OH)_{16}$AMBP reduces hydroxyapatite mineralization by 50% at a concentration of 1 μM, following a non-Langmuirian mechanism. Parallel studies with $C_{60}(OH)_{30}$ also indicate an affinity for hydroxyapatite, but at a reduced level (28% crystal growth rate reduction at 1 μM) compared with $C_{60}(OH)_{16}$AMBP. This study is the first to demonstrate that a fullerene-based material can be successfully targeted to a selected tissue as a step toward the development of such materials for medical purposes, in general.

Introduction

Fullerene- and metallofullerene-based materials offer promise as new diagnostic and therapeutic drugs.[1] This promise is based on the facts that such materials are proving to be relatively non-toxic,[2–5] non-metabolizable,[6] and capable of in vivo delivery of radiolabeled and non-labeled metal ions commonly used in diagnostic and therapeutic medicine. To fulfill their promise, however, such materials must also be capable of being selectively delivered to specific tissue upon demand.

Bone tissue is an especially appealing target for vectored pharmaceuticals because its primary inorganic component, hydroxyapatite (HAP), offers a multitude of binding sites for structurally suitable compounds. Compounds with functional groups such as hydroxyls and carboxylic and phosphonic acids are capable of forming ionic and hydrogen bonds to the mineral portion of bone.[7–9] The interactions between a bone-vectored compound and the mineralized tissue may be modeled in vitro using HAP crystal growth inhibition studies,[10–12] whereby compounds with high affinity for HAP bind to the surface of the crystals at kinks and dislocations, blocking crystallization. Using carefully designed experiments, the extent of crystal growth inhibition by a bone-vectored compound can then be used to estimate the compound's affinity for bone tissue in vivo.[13]

Crystal growth inhibition technology is especially important because bone-vectored compounds typically target areas of bone undergoing formation and resorption processes.[14] The vectored compounds are attracted to the active growth sites of HAP, and thus bind in greatest concentration to the metabolically-active portions of bone. Where bone tissue is diseased, a high rate of bone metabolism exists, and this activity attracts suitably-derivatized compounds to the diseased site. If, for instance, a radionuclide-containing fullerene derivative[15] could be successfully vectored to these diseased sites in bone, an opportunity exists for tissue-specific radiation therapy. High tissue specificity reduces the dose level required by the subject, and thereby reduces treatment costs and potential harm to non-diseased tissues. As yet, no tissue-vectored fullerene derivatives have been reported. This study is the first to specifically target a fullerene-based material to a particular tissue type with a bisphosphonate-C_{60} derivative, $C_{60}(OH)_{16}$AMBP (Fig. 1), being targeted to mineralized bone in vitro.

*Corresponding author. Tel.: +1-713-348-3268; fax: +1-713-348-5155; e-mail: durango@rice.edu

0968-0896/02/$ - see front matter
PII: S0968-0896(02)00049-4

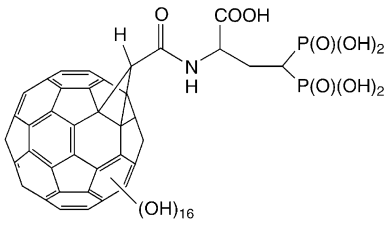

Figure 1. $C_{60}(OH)_{16}$AMBP, the bone-vectored fullerene derivative.

Results and Discussion

Constant composition growth experiments were first performed in pure supersaturated solutions of HAP and then in the presence of $C_{60}(OH)_{16}$AMBP and $C_{60}(OH)_{30}$. The results are presented in Table 1.

Figures 2 and 3 show typical plots of titrant volume required to maintain the supersaturation as a function of time at different fullerene concentrations. For comparison, a curve of titrant consumption for the growth of HAP crystals in pure supersaturated solutions is included (open symbols). All the rate curves show a rapid titrant addition immediately following the introduction of seed crystals. This frequently observed phenomenon, usually attributed to conditioning of the surface of the seed crystals in the supersaturated solution, may reflect ion exchange involving solution and surface cations and protons, or the removal of active growth sites on the seed crystals due to the rapid crystallization of high energy sites.[16,17] Significant reductions of the initial surges observed in the presence of the fullerenes suggest their adsorption at the growth sites on the HAP seed crystals, thus their competition with other initial surface processes. It can be seen in Figure 2 that linearity of the rate plots of HAP crystal growth (reflected by the constant slopes of volume versus time curves) was usually achieved 10–20 min after seed introduction to the supersaturated solution in experiments performed in the absence and presence of fullerenes. It should be noted that at high concentrations of inhibitors, HAP crystals appear to grow only during the initial reaction stage.

It is quite well established that strong inhibitors of crystal growth, such as the phosphonates, act by blocking, through adsorption, active growth sites at the crystal surfaces.[16,18] Commonly, inhibition kinetics data are interpreted in terms of a simple Langmuir adsorption model. Assuming that the adsorbed fullerene molecules occupy a fraction, θ, of the active growth sites, thereby preventing them from participating in the growth, the growth rate R can be written in terms of the uninhibited rate R_0 (eq 2)

$$R_0/R = 1 + K_L C \quad (2)$$

in which K_L is the adsorption affinity constant with units of liters per mole. Crystal growth rates R measured in the presence of $C_{60}(OH)_{30}$ and $C_{60}(OH)_{16}$AMBP are plotted in Figure 4 as a function of additive concentration.

Comparison of the two curves shows that both compounds inhibit HAP crystal growth, with $C_{60}(OH)_{16}$AMBP being the more effective inhibitor. At a concentration of 3.1×10^{-5} M, $C_{60}(OH)_{30}$ reduces the

Table 1. The rate of HAP crystallization decreases with increasing concentration of water-soluble fullerene derivatives

$C_{60}(OH)_{30}$ (10^{-6} mol L^{-1})	Rate (10^{-8} mol min^{-1} m^{-2})	$C_{60}(OH_{16}AMBP)$ (10^{-6} mol L^{-1})	Rate (10^{-8} mol min^{-1} m^{-2})
0	9.09	0	9.09
0.41	8.31	0.39	7.67
0.81	7.8	0.77	6.51
1.22	6.55	1.16	4.55
1.63	5.94	1.54	3.77
2.03	5.7	1.93	2.83
2.44	4.65	2.32	2.46
2.85	4.07	2.7	1.92
3.25	3.97	3.09	1.57
3.66	3.85	3.47	1.23
4.07	2.64		
4.47	2.49		

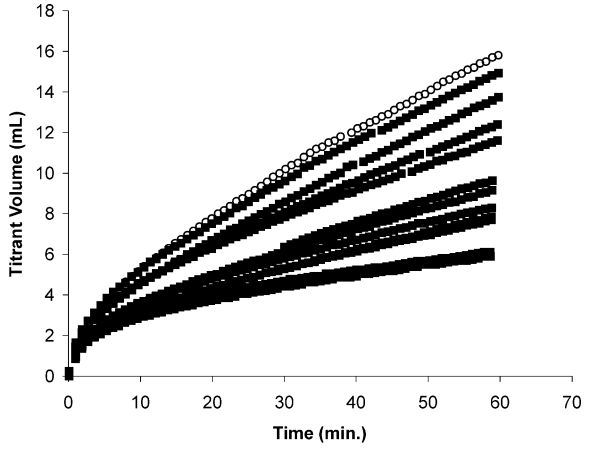

Figure 2. Titrant volume added as a function of time during constant composition HAP crystal growth inhibition experiments with $C_{60}(OH)_{30}$.

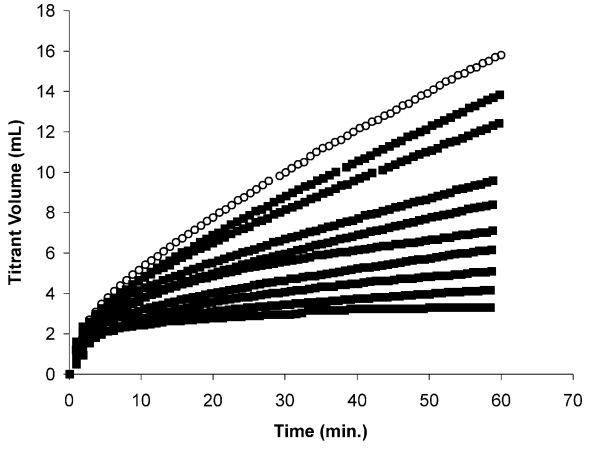

Figure 3. Titrant volume added as a function of time during constant composition HAP crystal growth inhibition experiments with $C_{60}(OH)_{16}$AMBP.

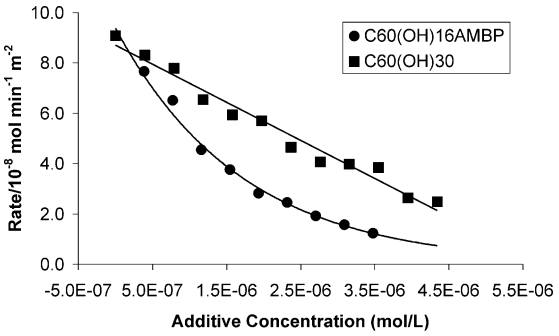

Figure 4. Rate of HAP crystal growth in the presence of $C_{60}(OH)_{30}$ (■) and $C_{60}(OH)_{16}AMBP$ (●).

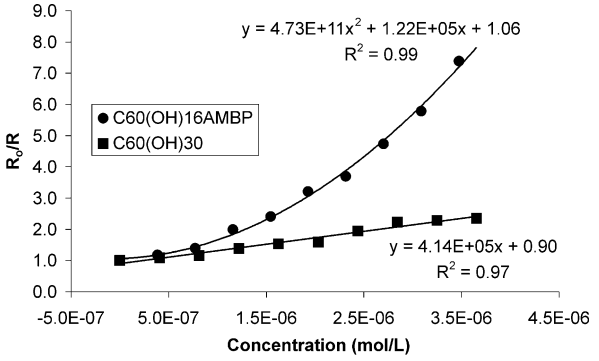

Figure 5. Plot of R_0/R versus concentration for $C_{60}(OH)_{30}$ (■) and $C_{60}(OH)_{16}AMBP$ (●).

HAP crystal growth by 58%, while $C_{60}(OH)_{16}AMBP$ reduces the rate by 87%. The increase in inhibition is linear with concentration for $C_{60}(OH)_{30}$, but not for the bisphosphonate derivative, $C_{60}(OH)_{16}AMBP$.

Following eq 2, plots of R_0/R as a function of concentration for each compound are shown below in Figure 5.

The linear relation shown for $C_{60}(OH)_{30}$ indicates that the compound inhibits HAP crystal growth by the mechanism described by the Langmuir formalism. From the slope, the affinity constant is 4.14 10^5 L mol^{-1} ($R^2 = 0.97$). In fact, this affinity of fullerenol materials for HAP has also been observed previously in an in vivo mouse model study using radiolabeled $^{166}Ho@C_{60}(OH)_x$.[15]

The plot of R_0/R versus concentration for $C_{60}(OH)_{16}AMBP$ lacks linearity, which suggests that the mechanism of inhibition is different from that described by the Langmuir model. The model relies on the assumptions that the inhibitor reversibly binds to the mineral surface at active growth sites and that the surface-bound molecules do not interact with one another.[16,19] For $C_{60}(OH)_{16}AMBP$, these assumptions may be invalid. The curvature observed in Figure 4 for $C_{60}(OH)_{16}AMBP$ at higher concentrations may be caused by lateral interference among the surface-bound molecules. Once adsorbed to a surface, molecules are capable of lateral movement and surface aggregation.

Table 2. Data from HAP crystal growth inhibition studies with $C_{60}(OH)_{30}$, $C_{60}(OH)_{16}AMBP$, and $CH_3C(OH)[P(O)(OH)_2]_2$

Compound	Concentration (mol/L)	Percent reduction in growth rate	Affinity constant (L mol^{-1})
$C_{60}(OH)_{30}$	1.0×10^{-6}	28	4.14×10^5
$C_{60}(OH)_{16}AMBP$	$1.\times10^{-6}$	50	—
$C_{60}(OH)_{16}AMBP$	3.5×10^{-6}	87	—
$CH_3C(OH)[P(O)(OH)_2]_2$	1.0×10^{-6}	69[a]	13.3×10^{5}[a]

[a]Ref 29.

Under such conditions, an equilibrium distribution may be impossible, thereby preventing the molecules from effectively inhibiting mineralization. In experiments with higher inhibitor concentrations, molecular aggregation can develop more easily, thus making the decrease in inhibitory activity more apparent. Such aggregation may result from enhanced intermolecular hydrogen bonding interactions among the hydroxyl and carboxylic and phosphonic acid groups of the fullerene material.

Table 2 compares the percent reductions in growth rate of the two fullerenol derivatives to that for 1-hydroxyethylidene-1,1-diphosphonic acid, $CH_3C(OH)[P(O)(OH)_2]_2$, a commercially-available bone-vectored compound used in the treatment of osteoporosis.[20] At 1.0×10^{-6} M inhibitor concentration, neither $C_{60}(OH)_{30}$ nor $C_{60}(OH)_{16}AMBP$ is as effective as $CH_3C(OH)[P(O)(OH)_2]_2$ at inhibiting HAP crystal growth. $C_{60}(OH)_{30}$ also has a lower affinity constant, suggesting that the compound binds to the surface less strongly than $CH_3C(OH)[P(O)(OH)_2]_2$. The lower binding constant for $C_{60}(OH)_{30}$ is not surprising given that the fullerenol does not contain a bisphosphonic acid moiety. The hydroxyl functionalities present in $C_{60}(OH)_{30}$ are capable of hydrogen bonding to the surface, but they do not provide the stronger ionic interactions that are present with bisphosphonic acid groups.

Comparison of $C_{60}(OH)_{16}AMBP$ to $CH_3C(OH)[P(O)(OH)_2]_2$ is somewhat problematic because the latter molecule inhibits HAP crystal growth by a mechanism that appears strictly Langmuirian, with the affinity constant being independent of concentration. As shown in Figure 4, such independence is not the case for $C_{60}(OH)_{16}AMBP$.

Despite uncertainty in the inhibition mechanism, the results demonstrate that both $C_{60}(OH)_{30}$ and $C_{60}(OH)_{16}AMBP$ inhibit HAP crystal growth from supersaturated calcium phosphate solutions and that both compounds have relatively strong affinities for HAP. The greater crystal growth inhibition by $C_{60}(OH)_{16}AMBP$ stresses the importance of incorporating bisphosphonate moieties into bone-vectored fullerene derivatives. Further explanation for the diminished rate inhibition observed at higher $C_{60}(OH)_{16}AMBP$ concentrations will require studies of other fullerene compounds, especially those having multidirectional surface-binding functionalities such as

$C_{60}C_6(COOH)_{12}$[21,22] and others. As the first investigation, however, the present study demonstrates the potential usefulness of fullerene-based materials in tissue-targeting technologies and lays the ground-work for in vivo studies using radiolabeled bisphosphonate materials as potential bone therapeutic agents.

Experimental

Materials

Reagent grade solvents and electrolytes (Fisher) were used without purification unless stated otherwise. Anhydrous solvents were obtained by distillation from appropriate drying agents under inert atmosphere. Petroleum ether and bromobenzene were each pre-dried with $NaSO_4$ and then refluxed over and distilled from sodium. Benzene, toluene, and ethyl ether were each pre-dried with $CaCl_2$ and then refluxed over and distilled from sodium in the presence of sodium benzophenone ketyl. Chloroform, stabilized with 0.75% ethanol, was used as received. Triethylamine was distilled from KOH under inert atmosphere.

Silica gel (Aldrich, grade 62, 60–200 mesh, 150 Å) was activated at 130 °C for a minimum of 12 h before use. Sephadex G-25 (Aldrich, 20–80 μ) was equilibrated in DI H_2O for 24 h at room temperature prior to use.

Physical and spectroscopic methods

Unless otherwise noted, residual solvent signals were used for spectral reference in the ^{13}C and ^{1}H NMR spectra (DMSO-d_6, 2.50 and 39.1 ppm; $CDCl_3$, 7.26 and 77.0 ppm; D_2O, 4.70 ppm). Phosphoric acid (85%, 0 ppm) was used as an external reference for ^{31}P NMR spectra. Signals that were shifted upfield from H_3PO_4 were assigned positive values; signals downfield from H_3PO_4 were assigned negative values. For each set of phosphorus NMR data, the upfield or downfield shift is stated for clarity.

Mass spectra were measured on a Finnigan MAT 95 GC-MS analyzer using electron ionization (EI, 70 eV) or atmospheric pressure chemical ionization (APCI). High-resolution APCI peak matching spectra were collected using Gramocidin S as the peak reference at 1141.71376 amu in 50/50 $CHCl_3$/MeOH.

Elemental analyses were obtained commercially from Galbraith Laboratories, Inc., Knoxville, TN, USA.

Materials and Methods for HAP crystal growth inhibition studies

Hydroxyapatite seed crystals were prepared from calcium nitrate and potassium dihydrogen phosphate, as detailed elsewhere.[23] The specific surface area, 34.9 $m^2\ g^{-1}$, was determined by BET nitrogen adsorption using a 30/70 N_2/He mixture (Monosorb, Quantachrome Corp). HAP crystals in the form of a suspension in water (41.8 g L^{-1}) were used for the crystal growth experiments.

Solutions were prepared using triply distilled carbon dioxide-free water and filtered before use through washed 0.22 μm filters (Millipore, Bedford, MA, USA). Calcium concentrations were determined either complexometrically by EDTA titration with Eriochrome Black-T as indicator, or by atomic absorption (Perkin-Elmer, model 3100, Norwich, CT, USA). Carbon dioxide-free potassium hydroxide solutions were prepared from washed reagent grade pellets in a nitrogen atmosphere.

Crystal growth experiments were made in magnetically-stirred water-jacketed Pyrex vessels at 37.0 ± 0.05 °C with ionic strength, I = 0.15 mol L^{-1}, adjusted by the addition of sodium chloride. Supersaturated solutions were prepared by introducing calcium chloride solution, followed by potassium dihydrogen phosphate solution. The pH was adjusted to the required value by the slow addition of potassium hydroxide solutions. During the reactions, carbon dioxide was excluded by bubbling with presaturated nitrogen gas. After equilibration, 0.5 mL of the HAP slurry was introduced to initiate the reaction. Since the nucleation and growth of crystals consume solution lattice ions, the lowering of pH was used to trigger the addition of two titrant solutions that served to maintain constant the pH, the concentrations of calcium and phosphate and the ionic strength of the solution. A glass electrode (Orion, model 9101), standardized using two NBS buffer solutions at pH 7.386 and 4.028 at 37 °C, was used to control titrant addition through a potentiostat. The total calcium concentration in all experiments was 6.00×10^{-4} mol L^{-1} with a calcium/phosphate molar ratio of 1.67, so as to achieve a supersaturation with respect to HAP of $\sigma = 5.55$ (as defined in eq 1), as computed from mass balance, proton dissociation, electroneutrality, and equilibrium expressions involving calcium and phosphate species.

$$\sigma = S - 1 = \left[IP/K_{SO}\right]^{1/v} - 1 \quad (1)$$

In eq 1, v is the number of ions per formula unit of precipitating phase and IP and K_{SO} are the ionic and solubility products, respectively, of HAP. The addition of the fullerene derivatives at micromolar levels to the reaction solutions did not affect the established supersaturation.

During the reactions, samples were withdrawn periodically, filtered (0.22 μm Millipore filter) and analyzed for calcium by atomic absorption and for phosphate spectrophotometrically (Varian, Cary 210) as the phosphovanadomolybdate complex in order to verify the constancy of the solution composition. Solid phases were examined by X-ray powder diffraction, XRD (Siemens Nicolet/Nic spectrometer, CuK radiation with Ni filter = 1.540; 2 from 3 to 45°), by scanning electron microscopy (SEM at 20 kV; JEOL JSM-5300, Noran Instrumental Inc. Middleton, WI, USA) and by diffuse reflectance infrared Fourier transform spectroscopy (FTIR, Perkin-Elmer 1760X FT-IR spectrometer). Plots of mineralization were calculated from plots of titrant volumes as a function of time as described previously.[23]

In order to investigate the uptake of fullerene derivatives by HAP surfaces, an equilibrium adsorption experiment was performed in which 0.0209 g of HAP in its saturated solution was equilibrated with various concentrations of these additives. A UV–visible spectrophotometer (Perkin-Elmer model 3100) was used for the analysis of fullerene derivative concentrations. Since the ζ-potential of HAP surfaces was markedly influenced by the presence of the additives, this parameter was used as an indication of the extent of adsorption. The ζ-potential of HAP surfaces for the same suspensions in the presence of these additives was measured using a Malvern Zetasizer IIc (Malvern, UK).

Syntheses

1,2-Dihydro-1,2-methanofullerene[60]-61-carboxylic acid, C_{60}-CHCOOH. 1,2-Dihydro-1,2-methanofullerene[60]-61-carboxylic acid was synthesized according to the procedure by Isaacs and Diederich.[24]

Tetraethyl ethenylidenebisphosphonate. In a typical synthesis,[25] paraformaldehyde (2.60 g, 86.7 mmol) and diethylamine (1.79 mL, 1.27 g, 17.4 mmol) were combined in MeOH (25 mL) with gentle warming to aid dissolution. The mixture was then cooled to room temperature and 5.0 g (17.3 mmol) tetraethyl methylenediphosphonate was added with stirring. The reaction was refluxed for 24 h under atmospheric conditions and then diluted with 25 mL MeOH and concentrated under vacuum at 35 C. Toluene (50 mL) was added to the flask and the contents were again concentrated under vacuum at 35 C. This step was repeated a second time to ensure that all of the MeOH had been removed. The intermediate (tetraethyl 2-methoxyethylenebisphosphonate) was then placed under vacuum at room temperature for 3 h. ^{1}H NMR (250 MHz, $CDCl_3$) δ 4.15 (m, 8H), 3.84 (td, 2H, $J_{P\text{-}H}=16.3$ Hz, $J_{H\text{-}H}=5.4$ Hz), 3.33 (s, 3H), 2.65 (tt, 1H, $J_{P\text{-}H}=23.8$ Hz, $J_{H\text{-}H}=5.4$ Hz), 1.30 (t, 12H, $J=7.0$ Hz).

The reaction flask was attached to a septum-capped soxlet extractor containing 4 Å molecular sieves and the entire system was flushed with Ar for 15 min. Approximately 125 mL anhydrous toluene was then added through the condenser. *p*-Toluenesulfonic acid monohydrate (0.20 g, 1.1 mmol) was added under Ar sparge and the flask was wrapped with aluminum foil. The reaction was refluxed under inert atmosphere for 14 h. After solvent removal, the remaining light yellow oil was redissolved in $CHCl_3$, washed with three 50 mL portions of DI H_2O, and dried over $MgSO_4$. The $CHCl_3$ was then removed, leaving a yellow oil that distilled over at 139 C/1 torr as a colorless liquid. An analytically pure sample was prepared by column chromatography on SiO_2 with 50:50 hexanes/acetone eluent. Yield: 4.0 g, 77%. ^{1}H NMR (250 MHz, $CDCl_3$) δ 6.96 (distorted dd, $J_{P\text{-}H}=37.6$ Hz, $J_{P\text{-}H}=34.1$ Hz), 4.14 (m, 8H), 1.33 (t, $J_{H\text{-}H}=7.1$ Hz, 12H); ^{13}C NMR (250 MHz, $CDCl_3$, TMS ref) δ 149.28, 131.80 (t, $J_{P\text{-}C}=166.5$ Hz), 62.60 (t, $J_{P\text{-}C}=2.8$ Hz), 16.20 (t, $J_{P\text{-}C}=3.3$ Hz); ^{31}P NMR (250 MHz, $CDCl_3$) 13.73 ppm downfield from H_3PO_4. IR (neat): 2984 (C–H), 2935 (C–H), 2910 (C–H), 1636 (C=C), 1251, (P=O), 1024 (C–O), 974 (P–C–P bend), 803 cm^{-1} (P–O).

Benzylidene glycine ethyl ester. In a typical synthesis,[26] the hydrochloride salt of glycine ethyl ester (15.0 g, 107.5 mmol) was dissolved in 125 mL CH_2Cl_2. Treatment with freshly distilled NEt_3 (21.8 g, 30 mL, 215.8 mmol) resulted in the formation of a small amount of white precipitate. Benzaldehyde (7.60 g, 7.28 mL, 71.6 mmol) was then added to the reaction at room temperature followed by 6 g $MgSO_4$ to remove the water by-product. After 10 h stirring, the solution was filtered and reduced under vacuum to give a yellow oil. This compound was dissolved in 100 mL Et_2O, washed with satd aq NaCl (6×50 mL) and dried ($MgSO_4$). Solvent removal under vacuum at 25 °C gave a light yellow oil that was used without further purification. The compound was stored at 10 °C. Yield: 13.42 g, 98%. ^{1}H NMR (250 MHz, $CDCl_3$, TMS ref) δ 8.30 (s, 1H), 7.78 (m, 2H), 7.42 (m, 3H), 4.40 (s, 2H), 4.24 (q, 2H, $J=7.1$ Hz), 1.31 ppm (t, 3H, $J=7.1$ Hz); ^{13}C NMR (250 MHz, $CDCl_3$) δ 169.99, 165.27, 135.45, 131.07, 128.46, 128.35, 61.94, 60.94, 14.07. IR (neat): 3063 (Ar C–H), 3029 (Ar C–H), 2983 (C–H), 2938 (C–H), 2975 (C–H), 2903 (C–H), 2854 (C–H), 1735 (C=O), 1646 (C=N), 1200 (C–O), 1027 (C–O), 759 (Ar–H out-of-plane), 694 cm^{-1} (Ar–H out-of-plane).

Ethyl *N* - benzylidene - 2 - amino - 4,4 - bis(diethoxyphosphoryl)butyrate. In a typical synthesis,[27] benzylidene glycine ethyl ester (1.91 g, 10.0 mmol) was added to a solution of NaOEt (1 mmol) in 20 mL of fresh absolute EtOH at −8 °C (ice-salt bath). Tetraethyl ethenylidenebisphosphonate (3.00 g, 10.0 mmol) was added dropwise over 3 min with vigorous stirring. The reaction was stirred for 30 min at 25 °C and then neutralized with satd aq NH_4Cl (ca. 3 mL). Removal of the EtOH (ca. 25 °C) at reduced pressure left a paste-like residue that was extracted with $CHCl_3$ (3×20 mL). The organic fraction was dried over $MgSO_4$, filtered and evaporated at reduced pressure to give a light-yellow oil that was stored in the freezer. Yield: 4.72 g, 96%. ^{1}H NMR (250 MHz, $CDCl_3$, TMS ref) δ 8.38 (s, 1H, N=C*H*Ph), 7.76 (m, 2H), 7.44 (m, 3H), 4.46 (dd, 1H, $J=4.9$, 8.8 Hz), 4.16 (m, 10H), 2.7–2.3 (m, 3H), 1.32 (m, 15H); ^{13}C NMR (250 MHz, $CDCl_3$) δ 171.08, 165.47, 135.54, 131.18, 128.49, 128.44, 69.81 (dd, $J=4.4$, 10.5 Hz), 62.5 (m), 61.11, 32.73 (t, $J=133.1$ Hz), 28.83, 16.30 (d, $^3J_{C\text{-}P}=24.3$ Hz), 14.05; ^{31}P NMR (250 MHz, $CDCl_3$): 23.66, 23.93 ppm, downfield from H_3PO_4. IR (neat): 2984 (C–H), 2933 (C–H), 2907 (C–H), 2872 (C–H), 1737 (ester C=O), 1641 (CH=N), 1280 (shoulder; P=O), 1253 (P=O), 1027 (C–O), 970 (P–C–P), 754 cm^{-1} (P–O).

Ethyl 2-amino-4,4-bis(diethoxyphosphoryl)butyrate. In a typical synthesis,[27] ethyl *N*-benzylidene-2-amino-4,4-bis(diethoxyphosphoryl)butyrate (3.00 g, 6.1 mmol) was dissolved in 10 mL DI H_2O at room temperature. *p*-Toluenesulfonic acid monohydrate (1.74 g, 9.2 mmol) was then added and the mixture was stirred for 30 min at room temperature. After extraction with Et_2O (4×15

mL) to remove benzaldehyde, the aqueous solution was rendered alkaline by addition of satd aq $NaHCO_3$ (ca. pH 8.1) and then extracted with $CHCl_3$ (4×10 mL). The organic layer was dried over $MgSO_4$, filtered and evaporated under reduced pressure to give a light yellow oil that was used without further purification. The compound was stored in the freezer and checked by NMR to ascertain purity before each use. Yield: 2.3 g, 94%. ^{1}H NMR (200 MHz, $CDCl_3$, TMS ref) δ 4.2 (m, 10H), 3.77 (dd, J=4.4, 10.6 Hz, 1H), 3.14–2.84 (dddd, $^3J_{HH}$=3.3 Hz, $^3J'_{HH}$=8.9 Hz, $^2J_{HP}$=23.2 Hz, and $^2J'_{HP}$=24.7 Hz, 1H, PC*H*P), 2.5–2.2 (m, 1H), 2.1–1.8 (m, 1H), 1.3 (m, 15H); ^{13}C NMR (200 MHz, $CDCl_3$) δ 175.50, 62.5 (m), 61.02, 52.77 (dd, J=10.3, 3.1 Hz), 32.77 (t, J=133.9 Hz), 30.49, 16.39 (d, J=6.1 Hz), 14.22; ^{31}P NMR (250 MHz, $CDCl_3$,): 24.43, 24.16 ppm, downfield from H_3PO_4. IR (neat): 3476 (br, N–H), 2984 (C–H), 2934 (C–H), 2910 (C–H), 1733 (ester C=O), 1646 (NH_2 deformation), 1277 (shoulder, P=O), 1245 (P=O), 1020 (C–O), 972 (P–C–P), 838 (P–O), 799 cm^{-1} (P–O).

Ethyl 4,4-bis(diethoxyphosphoryl)-2-(1,2-dihydro-1,2-methanofullerene[60]-61-carboxamido)butyrate, C_{60}AMBP-protected. C_{60}-CHCOOH (0.100 g, 0.128 mmol) and 1-hydroxybenzotriazole, BtOH, (0.035 g, 0.256 mmol) were combined in 30 mL PhBr. Approximately 0.104 g (0.256 mmol) ethyl 2-amino-4,4-bis(diethoxyphosphoryl)butyrate, AMBP, was added via pipette. Immediately, 0.0530 g (0.256 mmol) 1,3-dicyclohexylcarbodiimide (DCC) was added to the reaction flask. Stirring for 5 days at room temperature under inert atmosphere yielded a dark cranberry colored solution. The product was purified by column chromatography on a 10×1 inch SiO_2 column using toluene to elute PhBr and a 1% MeOH/$CHCl_3$ solution to elute the cranberry colored product. Two precipitations from $CHCl_3$ with Et_2O gave a brown solid that was collected in a centrifuge tube and dried overnight under vacuum at room temperature. Yield: 0.103 g, 69%. ^{1}H NMR (200 MHz, $CDCl_3$) δ 8.93 (br d, 1H, J=7.8), 4.85 (m, 1H), 4.79 (s, 1H), 4.27 (m, 10H), 2.71–2.46 (m, 3H), 1.43 (m, 15H); ^{13}C NMR (200 MHz, $CDCl_3$) δ 170.74, 165.37, 34 out of 60 fullerene resonances observed −148.53, 148.36, 146.48, 146.17, 145.59, 145.50, 145.08, 144.89, 144.80, 144.61, 144.43, 144.31, 144.24, 144.02, 143.76, 143.70, 143.49, 143.44, 143.10, 142.86, 142.77, 142.72, 142.55, 142.24, 141.98, 141.91, 141.85, 140.87, 140.58, 140.20, 140.10, 136.20, 136.10, 71.56 (2×; sp^3 C_{60} bridgehead carbon atoms), 63.33 (m), 61.93, 53.13, 41.11, 33.34 (t, J=132.1 Hz), 26.72 (br s), 16.48 (br d), 14.23; ^{31}P NMR (400 MHz, $CDCl_3$, H_3PO_4): 24.51 (d, J=5.2 Hz), 24.48 ppm downfield from H_3PO_4 (d, J=5.2 Hz). IR (KBr): 3244 (N-H), 2977 (C–H), 2900 (C–H), 1734 (carboxy ester C=O), 1684 (amide I band), 1540 (amide II band), 1249 (P=O), 1023 (C–O), 972 (P–C–P), 798 (P–O) 528 cm^{-1} (fullerene stretch). UV–vis ($CHCl_3$, λ nm, (ε M^{-1} cm^{-1})): 326 (3.4×10^4), 402 (4.1×10^3), 416 (3.4×10^3), 427 (3.7×10^3), 479 (1.7×10^3), 690 (2.1×10^2). High res. APCI-MS (50:50 $CHCl_3$/MeOH): 1164.153200 ($M^+ + 1$). Anal. Calcd for $C_{76}H_{31}NO_9P_2$: C, 78.42; H, 2.68; N, 1.20; O, 12.37; P, 5.32. Found: C, 77.42; H, 3.19; N, 1.19; (O, 12.89); P, 5.31.

4,4 - Bisphosphono - 2 - (1,2 - dihydro - 1,2 - methanofullerene[60]-61-carbox-amido)butyric acid, C_{60}AMBP. C_{60}-AMBP-protected (0.160 g, 0.137 mmol) was dissolved in 125 mL anhydrous toluene in a glove box. I-Si$(CH_3)_3$[28] (0.196 mL, 0.275 g, 1.37 mmol) was added drop-wise at room temperature over 30 s. After 72 h stirring at 50 °C, the reaction was filtered to remove a dark insoluble product. The filtrate was then removed from the glove box and quenched with 1 mL MeOH. An insoluble brown precipitate formed immediately. It was collected in a centrifuge tube, washed consecutively with $CHCl_3$ and Et_2O, and then dried under vacuum at 65 °C for 8 h. This compound was insoluble in all common solvents. Yield: 127 mg, 90%. IR (KBr): 3600–2500 (br, P–OH), 2923 (C–H), 1719 (acid C=O), 1650 (amide I band), 1540 (amide II band), 1241–1024 (envelope P=O, C–O, OH bend), 928 (P–C–P), 526 cm^{-1} (fullerene resonance).

The intermediate tetra-silyl ester, produced by the reaction of ITMS with the four phosphonate ester groups was characterized by ^{1}H NMR. ^{1}H NMR (200 MHz, CD_2Cl_2) δ N*H* not observed, 5.26 (s, 1H), 5.04 (m, 1H), 4.37 (q, 2H), 2.75–2.15 (br m, 3H), 1.35 (t, 3H), 0.52 and 0.43 (br s, 36H). CH_3CH_2I is also present in the sample as a by-product of the deprotection reaction.

4,4-Bisphosphono-2-(polyhydroxyl-1,2-dihydro-1,2-methanofullerene[60]-61-carboxamido)butyric acid, $C_{60}(OH)_{16}$-AMBP. A less vigorous hydroxylation procedure was used for $C_{60}(OH)_{16}$AMBP than for C_{60}(below) to ensure survival of the bisphosphonate substituent. C_{60}AMBP (0.050 g, 0.05 mmol) was dissolved in 0.5 mL 40% tetra *n*-butylammonium hydroxide and then diluted to 10 mL with 1 M KOH. The mixture was stirred for 24 h at room temperature and then chromatographed on Sephadex G-25 (fine) size exclusion gel (2.5 inches×5 inches). The product eluted as a well-defined brown-orange band followed later by a volume of colorless basic eluent. Between aliquots, the column was rinsed thoroughly with DI H_2O until the pH of the eluent was no longer basic. After three passes, the pH of the collected sample fractions was ca. 6, suggesting that most of the base had been removed. The collected fractions were reduced to 10 mL under vacuum with *very* gentle heating (T<30 °C) and then dried under slow air flow overnight to remove the remaining solvent. The resulting flaky, black solid was collected and dried at 100 °C/1 torr over P_2O_5 for 12 h. 37 mg $C_{60}(OH)_{16}$AMBP isolated. ^{1}H NMR (250 MHz, D_2O) δ 4.15, 3.95, 3.56, 2.25, 1.9–0.9 (all br signals); ^{31}P NMR (250 MHz, D_2O): 12.4 ppm upfield from H_3PO_4 (br *weak* singlet). IR (KBr): 3358 (v br, O-H), 2922 (aliphatic C–H), 1717 (shoulder, carboxy C=O), 1595 (v br, amide C=O), 1387 (v br, O-H bend), 1239 (P=O), 1072 (s, C–O), 1045 (s, C–O). UV–vis (H_2O): No maxima were observed; the absorption curve decreases gradually toward the visible region. To describe the absorption strength, measurements were taken at 300, 400, and 500 nm. The molar extinction coefficients at these wavelengths are 22.9×10^6, 7.57×10^6 and 2.08×10^6 cm^2/mol, respectively. MALDI-MS: no peaks observed other than 720 (C_{60}). Anal. Calcd for $C_{66}H_{27}NO_{25}P_2$ ($C_{60}(OH)_{16}$AMBP) C, 61.18; H, 2.10; N, 1.09; P, 4.78;

O, 30.87. Found: C, 60.38; H, 2.77; N, 1.27; P, 4.86; (O, 30.72 by difference). Analysis for potassium showed only a trace amount (<0.37%).

Fullerenol[60], $C_{60}(OH)_{30}\cdot 2H_2O$. In a typical fullerenol synthesis,[29] 20 mg (2.7×10^{-5} mol) C_{60} (99.5%) was dissolved in a minimal volume of toluene (ca. 20 mL), using sonnication to encourage dissolution. This solution was then stirred vigorously with 10 mL concentrated KOH (ca. 1 g/mL) and three drops tetra-*n*-butylammonium-hydroxide (TBAH) phase transfer catalyst. Decoloration of the toluene layer occurred within min accompanied by formation of a black semi-solid at the solvent interface. The toluene layer was carefully decanted and the remaining water layer was sonnicated briefly and then stirred under air sparge at room temperature for 10–12 h to allow further reaction and to remove remaining toluene. Deionized water was then added to the remaining solution or solid to bring the total volume to 25 mL. The resulting suspension was stirred for 24–48 h to ensure complete reaction. The resulting orange-brown solution was diluted with an additional 10 mL DI H_2O and then vacuum filtered through Celite on a Büchner funnel to remove a small amount of insoluble material. The filtrate was concentrated under reduced pressure with gentle warming until precipitate started to form. MeOH was then added to complete precipitation. A mixture of brown and white solids was collected by centrifugation. The solids were redissolved in a minimal amount of water and again precipitated with MeOH to remove additional KOH and TBAH impurities. This step was repeated a third time. After the final precipitation, the compound was chromatographed on Sephadex G-25 (fine) size-exclusion gel. Two bands were observed: the first broad, orange band was collected while the second brown-orange band, being strongly basic, was discarded. The collected eluent was concentrated and precipitated with MeOH. If a pH measurement of the mother liquor indicated presence of base (if the pH >6 when saturated with CO_2), the compound was further purified. UV–vis: No maxima were observed; the absorption curve decreases gradually toward the visible region. To describe the absorption strength, measurements were taken at 300, 400, and 500 nm. The molar extinction coefficients at these wavelengths are 29.3×10^6, 9.7×10^6 and 2.6×10^6 cm^2/mol, respectively. Anal. calcd for $C_{60}H_{30}O_{30}\cdot 2H_2O$, $[C_{60}(OH)_{30}\cdot 2H_2O]$ C, 56.88; H, 2.71; O, 40.41. Found: C, 56.54; H, 2.53; (O, 40.93 by difference).

Acknowledgements

The Robert A. Welch Foundation (Grant C-0627) is gratefully acknowledged for support of this work. K.A.G. also thanks the National Institutes of Health for support through a biotechnology training fellowship and Dr. F.F. (Russ) Knapp Jr. for helpful discussions.

References and Notes

1. Wilson, L. J. *Electrochemical Society Interface* **1999**, *8*, 24.
2. Nelson, M. A.; Domann, F. E.; Bowden, G. T.; Hooser, S. B.; Fernando, Q.; Carter, D. E. *Toxicol. Ind. Health* **1993**, *9*, 623.
3. Baierl, T.; Drosselmeyer, E.; Seidel, A.; Hippeli, S. *Exp. Toxic. Pathol.* **1996**, *48*, 508.
4. Ueng, T.-H.; Kang, J.-J.; Wang, H.-W.; Cheng, Y.-W.; Chiang, L. Y. *Toxicol. Lett.* **1997**, *93*, 29.
5. Chen, H. H. C.; Yu, C.; Ueng, T. H.; Chen, S.; Chen, B. J.; Huang, K. J.; Chiang, L. Y. *Toxicol. Pathol.* **1998**, *26*, 143.
6. Moussa, F.; Pressac, M.; Hadchouel, M.; Arbeille, B.; Chretien, P.; Trivin, F.; Ceolin, R.; Szwarc, H. In *Recent Advances in the Chemistry and Physics of Fullerenes and Related Materials*; Kadish, K. M., Ruoff, R. S., Eds.; Proc. Electrochem. Soc. 97–42; Electrochemical Society: Pennington, NJ, 1997; Vol. 5, p 332.
7. Orme, M. W.; Labroo, V. M. *Bioorg. Med. Chem. Lett.* **1994**, *4*, 1375.
8. Willson, T. M.; Charifson, P. S.; Baxter, A. D.; Geddie, N. G. *Bioorg. Med. Chem. Lett.* **1996**, *6*, 1043.
9. Meyer, J. L.; Nancollas, G. H. *Calcif. Tissue Res.* **1973**, *13*, 295.
10. Nancollas, G. H.; Amjad, Z.; Koutsoukos, P. In *Chemical Modeling in Aqueous Systems: Speciation, Sorption, Solubility, Kinetics*; Jenne, E. A., Ed.; ACS Symposium Series; American Chemical Society: Washington, DC, 1979; Vol. 93, p 475.
11. Tomson, M. B.; Nancollas, G. H. *Science* **1978**, *200*, 1059.
12. Koutsoukos, P.; Amjad, Z.; Tomson, M. B.; Nancollas, G. H. *J. Am. Chem. Soc.* **1980**, *102*, 1553.
13. Francis, M. D.; Martordam, R. R. In *The Role of Phosphonates in Living Systems*; Hilderbrand, R. L., Ed.; CRC: Boca Raton, 1983; p 55.
14. Rodan, G. A.; Fleisch, H. A. *J. Clin. Invest.* **1996**, *97*, 2692.
15. Cagle, D. W.; Kennel, S. J.; Mirzadeh, S.; Alford, J. M.; Wilson, L. J. *Proc. Natl. Acad. Sci. U.S.A.* **1999**, *96*, 5182.
16. Zhang, J.-W.; Nancollas, G. H. In *Miner.-Water Interface Geochem.*; Hochella, M. F., White, A. F., Eds.; Reviews in Mineralogy; Mineralogical Society of America: Washington, DC, 1990; Vol. 23, p 365.
17. Zieba, A.; Nancollas, G. H. *J. Cryst. Growth* **1994**, *144*, 311.
18. Jancic, S. J.; De Long, E. J., Eds. *Industrial Crystallization*; Elsevier: Amsterdam, 1984.
19. Richardson, C. F. PhD Thesis, SUNY, Buffalo, NY, USA, 1991.
20. Amjad, Z. *Langmuir* **1987**, *3*, 1063.
21. Lamparth, I.; Hirsch, A. *J. Chem. Soc., Chem. Commun.* **1994**, 1727.
22. Lamparth, I.; Maichle-Moessmer, C.; Hirsch, A. *Angew. Chem., Int. Ed. Engl.* **1995**, *34*, 1607.
23. Ebrahimpour, A.; Johnsson, M.; Richardson, C. F.; Nancollas, G. H. *J. Colloid Interface Sci.* **1993**, *159*, 158.
24. Isaacs, L.; Diederich, F. *Helv. Chim. Acta* **1993**, *76*, 2454.
25. Degenhardt, C. R.; Burdsall, D. C. *J. Org. Chem.* **1986**, *51*, 3488.
26. Stork, G.; Leong, A. Y. W.; Touzin, A. M. *J. Org. Chem.* **1976**, *41*, 3491.
27. Sturtz, G.; Guervenou, J. *Synthesis* **1991**, 661.
28. Olah, G.; Narang, S. C. *Tetrahedron* **1982**, *38*, 2225.
29. Li, J.; Takeuchi, A.; Ozawa, M.; Li, X.; Saigo, K.; Kitazawa, K. *J. Chem. Soc., Chem. Commun.* **1993**, 1784.